IBRACON Structures and Materials Journal
Revista IBRACON de Estruturas e Materiais
ISSN 1983-4195 ismj.org

ORIGINAL ARTICLE

Reliability-based design optimization of a concrete dam

Otimização de projeto baseada em confiabilidade de uma barragem de concreto

Adrian Torrico Siacara[a,d]
Giovanni Pais Pellizzer[b]
André Teófilo Beck[c]
Marcos Massao Futai[a,d]

[a]Universidade de São Paulo – USP, Departamento de Engenharia de Estruturas e Geotécnica – PEF, São Paulo, SP, Brasil
[b]Universidade Federal de Mato Grosso do Sul – UFMS, Faculdade de Engenharias, Arquitetura e Urbanismo e Geografia, Campo Grande, MS, Brasil
[c]Universidade de São Paulo – USP, Departameto de Engenharia de Estruturas, São Carlos, SP, Brasil
[d]Universidade de São Paulo – USP, Grupo de Pesquisa GeoInfraUSP, São Paulo, SP, Brasil

Received 26 August 2021
Acepted 24 January 2022

Abstract: Performance and safety of geotechnical structures are affected by uncertainties. Yet, the design of dams is nowadays still made using deterministic methods and design codes. Dam optimization in a deterministic setting may lead to compromised safety margins. In this setting, Reliability-Based Design Optimization (RBDO) appears as an alternative, allowing one to optimize dam performance, but respecting specified reliability constraints. In this paper, we employ an efficient and accurate Single-Loop Approach (SLA) in the RBDO of a concrete dam. Considering dam equilibrium reliability constraints, we find the optimal dam base and optimal placement of drainage galleries, for different dam heights and different target reliability index (β_T). We show how the governing failure mode changes for each optimal solution: for large β_T, sliding limit state is the active constraint; for smaller β_T values, the eccentricity limit state function is found to be the active constraint for the optimum dam. We also investigate how the importance of random parameters change for each optimum solution: for large β_T and failure controlled by sliding, the cohesion and friction angle along dam base interface with foundation rock are the most relevant uncertain parameters for dam equilibrium. For smaller β_T with failure controlled by eccentricity, the more relevant uncertain geotechnical parameters are the base length of the dam, the specific weight of concrete, and the coefficient of drainage gallery inefficiency.

Keywords: reliability-based design optimization, concrete dam, reliability index, dam design, single-loop approach.

Resumo: O desempenho e a segurança das estruturas geotécnicas são afetados por incertezas. No entanto, o projeto de barragens ainda hoje é feito usando métodos determinísticos e códigos de projeto. A otimização da barragem em um cenário determinístico pode levar a margens de segurança comprometidas. Nesse cenário, a Otimização de Projeto Baseada em Confiabilidade (RBDO) surge como uma alternativa, permitindo otimizar o desempenho da barragem, mas respeitando as restrições de confiabilidade especificadas. Neste artigo, empregamos uma abordagem de loop único (SLA) eficiente e precisa no RBDO de uma barragem de concreto. Considerando as restrições de confiabilidade de equilíbrio da barragem, encontramos a base ótima da barragem e a localização ótima das galerias de drenagem, para diferentes alturas da barragem e diferentes índices de confiabilidade alvo (β_T). Mostramos como o modo de falha governante muda para cada solução ótima: para β_T grande, o estado limite de deslizamento é a restrição ativa; para valores menores de β_T, a função de estado limite de excentricidade é a restrição ativa para a barragem ótima. Também investigamos como a importância dos parâmetros aleatórios mudam para cada solução ótima: para grandes β_T e falhas controladas por deslizamento, a coesão e o ângulo de atrito ao longo da interface da base da barragem com a rocha de fundação são os parâmetros incertos mais relevantes para o equilíbrio da barragem. Para β_T menores com ruptura controlada por excentricidade, os parâmetros geotécnicos incertos mais relevantes são o

Corresponding author: Adrian Torrico Siacara. E-mail: adriantorricosiacara@gmail.com
Financial support: The Coordination for the Improvement of Higher Education Personnel (CAPES) (Grant number nº 88882.145758/2017-01) and the Brazilian National Council of Scientific and Technological Development (CNPq).
Conflict of interest: Nothing to declare.
Data Availability: The information required to reproduce findings of this study is reported in the paper. Other data such as computer codes will be made available by the corresponding author upon reasonable request.

comprimento de base da barragem, o peso específico do concreto e o coeficiente de ineficiência da galeria de drenagem.

Palavras-chave: otimização de projeto baseado em confiabilidade, barragem de concreto, índice de confiabilidade, projeto de barragem, abordagem de loop único.

How to cite: A. T. Siacara, G. P. Pellizzer, A. T. Beck, and M. M. Futai, "Reliability-based design optimization of a concrete dam", *Rev. IBRACON Estrut. Mater.*, vol. 15, no. 5, e15501, 2022, https://doi.org/10.1590/S1983-41952022000500001

1 INTRODUCTION

Geotechnical structures are designed under significant uncertainty in parameters. In concrete dams, the traditional approach for verifying stability is based on deterministic methods that use empirical safety factors (FS) or partial factors of safety for every failure mode. These empirical FS allow us to design conservative dams, without explicitly considering the uncertainties in geotechnical parameters. Different specialized standard agencies [1]– [8] and some authors [9], [10] give suggestions of minimum FS. These values determine if the structure has an acceptable level of safety or not. If minimum values are not met, the existing structures need to be strengthened and/or their use changed. In turn, the design procedure starts with an initial definition of the cross-section geometry, which is progressively updated until the safety criteria are met. However, these *FS* do not quantitatively measure the safety margin of the design and do not account for the influence of different design variables and their uncertainties on the overall system performance [11], [12].

Probabilistic methods can be employed to determine the probability of failure of a structure under different loading conditions. Probabilistic methods consider geotechnical parameters as random variables, which brings more confidence regarding the performance and safety of structures [13], [14]. In large dams, the development of national dam safety regulations was historically based on the classical approach (deterministic analysis). The ICOLD bulletin [15] encouraged theoretical investigations for the future adoption of a probabilistic approach to dam safety. This bulletin states that the logical trend, in the design phase, goes from the predominantly deterministic approach of global *FS* to the semi-probabilistic method of partial safety factors. For existing dams, the standards-based approach is recognized to be increasingly inadequate [16]. Due to their inherent conservatism, deterministic approaches may not be cost-effective for design of new dams, nor for safety evaluation of existing dams [17]. In those cases, the probabilistic approach has gained acceptance for the safety management of specific dams, for which the economic resources are very important. Reliability methods have been considered systematically to support decision-making regarding the operation or during the design of a dam.

In reliability theory, the first-order approximation to the probability of failure (P_f) is obtained by approximating the limit state at the design point by a hyperplane, which leads to (Equation 1):

$$P_f = \Phi(-\beta) \tag{1}$$

where $\Phi(.)$ is the standard Gaussian cumulative distribution function (CDF) and β is the reliability index [18]– [20]. The minimum distance of the limit state function to the origin of standard Gaussian space is the so-called reliability index (β), and the point over the limit state with minimum distance to the origin is called the "design point". By defining a target reliability index (β_T) with large distance to the failure domain, the chance of unsatisfactory performance can be reduced. In dam structures, β_T should be a function of the expected performance level [21]. Increasing the safety of structural systems usually implies additional costs, and sometimes cost savings can result in jeopardized safety [18]. The optimum design mostly involves a tradeoff between safety and economy [22].

Deterministic Design Optimization (DDO) allows finding the shape or configuration of a structure that is optimum in terms of mechanics, but the formulation grossly neglects parameter uncertainty and its effects on structural safety [23]. Consequently, a deterministic optimum design obtained without considering such uncertainties can result in an unreliable design [12]. Reliability-Based Design Optimization (RBDO) has emerged as an alternative to properly model the safety-under-uncertainty part of the problem. Uncertainties in geotechnical engineering come from loads, geotechnical properties, and calculation models [14], [24], [25]. The purpose of RBDO is to find a balanced design that is not only economic but also reliable in the presence of uncertainty [26]. With RBDO, one can ensure that a minimum (and measurable) level of safety is achieved by the optimum structure [23].

Although the idea of RBDO is attractive, its implementation is generally not easy because of the coupling between reliability assessment and cost minimization. Methods used to solve RBDO problems are usually classified into three groups [19], [27]:

(1) Bi-level RBDO approaches: reliability index approach (RIA) [28]– [30] and performance measure approach (PMA) [30], [31];
(2) Mono-level RBDO approaches: Single Loop Single Variable (SLSV) [32], Single Loop approach (SLA) [33], [34], Mono-Level RBDO [35], Reliable design space [36];
(3) Decoupled RBDO approaches: Traditional Approximation Method (TAM) [37], Sequential Optimization and Reliability Assessment (SORA) [38], Sequential Approximate Programming (SAP) [39], [40].

The above methods are very efficient for problems with linear and moderate nonlinear limit state functions. Traditionally, RBDO is conducted through the double-loop approach (also known as bi-level approach), in which the inner loop computes the reliability constraint, and the outer loop conducts the optimization. For this reason, the double-loop RBDO method is computationally expensive and, therefore, may be impractical for large-scale design problems.

Some studies have been carried out addressing RBDO of geotechnical structures in recent years. Chiti et al. [41] used subset simulation for RBDO of a concrete gravity dam. Zhao et al. [42] employed an Artificial Bee Colony (ABC) algorithm for RBDO analysis of retaining walls and spread footings. Zevgolis et al. [43] proposed a probabilistic geotechnical design optimization framework for large open-pit excavations. Zhao et al. [44] employed least square support vector machine (LSSVM) and artificial bee colony (ABC) algorithm for reliability-based support optimization of rock bolt reinforcement around tunnels. Santos et al. [45] used the FORM-based ant colony optimization (ACO) algorithm for reliability-based design optimization of geosynthetic-reinforced soil walls. Ji et al. [46] used the inverse FORM approach for reliability-based design in geotechnical engineering. Raviteja and Basha [47] presented a target reliability-based design optimization (TRBDO) approach of V-shaped anchor trenches for municipal solid waste landfills. Mahmood [11] used the FORM method with a minimization algorithm to illustrate the optimization of a retaining wall.

Using guidelines of specialized standards and considering uncertainties, this paper investigates the optimum location of gallery drainage and best geometry of a concrete dam using a mono-level Single-Loop Approach (SLA). We address a realistic dam design problem herein, but using analytical limit state functions. The combination of using analytical functions and an efficient single-loop optimization approach allows us to find the optimal dam base and optimal placement of drainage galleries, for different dam heights and different target reliability index. We also exploit how the governing failure mode changes as a function of the target reliability index (β_T) employed as design constraint, and as a function of dam height. We also investigate how the importance of random parameters change for each optimum solution.

The remainder of this paper is organized as follows. The basic formulation of RBDO is presented in Section 2. The application problem is described in Section 3. Implementation details of dam RBDO are described in Section 4. The results of the optimization analysis are presented and discussed in Section 5. Concluding remarks are presented in Section 6.

2 FORMULATION OF RELIABILITY-BASED OPTIMIZATION

2.1 Formulation of reliability analysis

Let $\mathbf{X} = \{X_1, X_2, \dots, X_n\}$ and $\mathbf{d} = \{d_1, d_2, \dots, d_n\}$ be vectors of structural system parameters. Vector $\mathbf{X} \in \mathbb{R}^{n_{RV}}$ contains n_{RV} random variables, and may include dimensions and geometry, resistance properties of materials or structural members, loads, and model error variables. Some of these parameters are random in nature; others cannot be defined deterministically due to uncertainty. Vector $\mathbf{d} \in \mathbb{R}^{n_{RV}}$ contains n_{DV} design variables whose values are to be determined to maximize the performance of the system, or to minimize weight, cost, etc. Typical variables in vector $\mathbf{d}$ are nominal member dimensions, partial safety factors, reinforcement ratio, design life, parameters of inspection and maintenance programs, etc.

The existence of uncertainty implies uncertainty in the performance of the structure, that is, the possibility of a structural failure. The boundary between safety and failure domain is given by limit state functions $g_i(\mathbf{d}, \mathbf{X})$, such that (Equation 2):

$$\mathrm{D}_{fi}(\mathbf{d}) = \{\mathbf{x} | g_i(\mathbf{d}, \mathbf{X}) \leq 0\},$$

$$\mathrm{D}_{si}(\mathbf{d}) = \{\mathbf{x} | g_i(\mathbf{d}, \mathbf{X}) > 0\}, \qquad i = 1, \ldots, n_{LS}, \tag{2}$$

where $\mathrm{D}_{fi}(\mathbf{d})$ is the failure domain, D_{si} is the safety domain, and n_{LS} is the number of limit state functions. Each limit state describes one possible failure mode of the structure. The probability of structural failure, or probability of failure, for the i^{th} failure mode, is given by (Equation 3):

$$P_{fi} = P[g_i(\mathbf{d}, \mathbf{X}) \leq 0] = \int_{D_{fi}} f_{\mathbf{x}}(\mathbf{x})\, d\mathbf{x} \tag{3}$$

where $f_{\mathbf{x}}(\mathbf{x})$ represents the joint probability density function of the random variable vector **X** and the integral is carried out over the failure domain. The probabilities of failure for individual limit states can be evaluated using traditional structural reliability methods such as first- and second-order reliability methods (FORM and SORM), as well as by Monte Carlo simulation (SMC). For multiple limit states, system reliability techniques have to be employed [18]– [20].

2.2 Reliability-Based Design Optimization (RBDO)

The RBDO is the generic name given to (structural) optimization that explicitly takes uncertainties into account. When the formulation of optimization uses reliability constraints, one obtains what has been called Reliability-Based Design Optimization (RBDO). A typical formulation reads (Equation 4):

Find $\mathbf{d}^*$ which minimizes $f(\mathbf{d})$

$$\text{Subject to: } P_{fi}(\mathbf{d}) \leq P_{fTi}, i = 1, \ldots, n_{LS}; \mathbf{d} \in \mathrm{S} \tag{4}$$

where $P_{fi}(\mathbf{d})$ is the failure probability for the i^{th} failure mode, P_{fTi} is the allowable failure probability for the i^{th} failure mode, n_{LS} is the number of limit states, and $\mathrm{S} = \{\mathbf{d}_{\min}, \mathbf{d}_{\max}\}$. The target safety or target reliability, for the i^{th} failure mode, is $r_{Ti} = \left(1 - P_{fTi}\right)$. Using reliability index β as the safety measure, Equation 4 can also be written as (Equation 5):

Find $\mathbf{d}^*$ which minimizes $f(\mathbf{d})$

$$\text{Subject to: } \beta_i(\mathbf{d}) \geq \beta_{Ti}, i = 1, \ldots, n_{LS}; \mathbf{d} \in \mathrm{S} \tag{5}$$

The main difference between RBDO and deterministic optimization is the introduction of uncertainties by considering them random variables instead of fixed values. A design with the RBDO process assures the safety of the structure when the parameters involved in the analysis are of random nature. In contrast, deterministic optimization cannot ensure the safety conditions [48]. An illustrative scheme of deterministic optimization (DO) and RBDO is depicted in Figure 1. In this figure two limit state functions are shown.

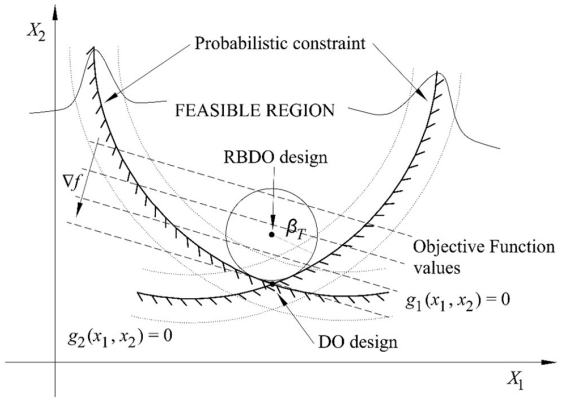

Figure 1. Illustrative scheme of deterministic optimization (DO) vs RBDO (based on [48]).

Failure probabilities or reliability indexes can be evaluated by classical structural reliability methods such as FORM, SORM, or SMC. However, the computational cost of evaluating these reliabilities needs to be considered, as reliability analysis is now performed within an optimization loop. Hence, structural reliability calculations must be repeated hundreds to thousand times. This will often require the use of specialized methods, which can reduce the overall computational burden [18]–[20].

The RBDO [49]–[51] is a natural extension of DDO, where deterministic constraints are replaced by probabilistic design constraints. RBDO does not account for the economic consequences of failure, since the safety level is a constraint, and not an optimization variable. DDO and RBDO can both be used to achieve mechanical structural efficiency. The safety-economy tradeoff is addressed by the risk optimization formulation [23], [28], [52]–[54], which is outside the scope of this study.

2.3 Single-Loop Approach (SLA)

The SLA method is a single-loop RBDO algorithm [33], [34], which operates by replacing the reliability constraint by the first-order optimality conditions. This method eliminates the need for inner reliability loops without increasing the number of design variables, as is the case with some other single-loop algorithms [55]– [57]. Concurrent convergence is thus obtained, whereby optimal design and target reliability are obtained simultaneously in the same optimization loop. SLA has been found to be more efficient, robust and accurate than many of the competing methods [27], [50].

SLA [33] approximates the design point of each reliability constraint by solving the first order Karush-Kuhn-Tucker (KKT) conditions for each iteration k. The formulation is given by (Equation 6):

Find $\mathbf{d}_{k+1}$ which minimizes $f(\mathbf{d})$

$$\text{Subject to: } g_i(\mathbf{d}, \mathbf{x}_{\text{ik}}) \geq 0, i = 1, \dots, n_{LS}; \mathbf{d} \in \text{S} \tag{6}$$

where vector $\mathbf{x}_{ik} = (\mu_{\mathbf{X}})_k - \left(\mathbf{J}_{xy}\right)_{ik} \boldsymbol{\alpha}_{ik} \beta_{Ti}$ is a linear approximation to the design point $\mathbf{x}_i^*$, at the k^{th} iteration, and vector $(\mu_{\mathbf{X}})_k$ needs to be updated only if random design variables are present. The Jacobian matrix $\mathbf{J}_{xy}$ of the transformation $\mathbf{x} = T^{-1}(\mathbf{y}) = \mathbf{J}_{xy}\mathbf{y} + \mu_{\mathbf{x}}$ is given by (Equation 7):

$$\mathbf{J}_{xy} = \left\{\frac{dx_l}{dy_m}\right\}_{l=1,\dots,n_{RV};m=1,\dots,n_{RV}} \tag{7}$$

The design point $\mathbf{y}_i^* = T(\mathbf{x}_i^*)$ is the point over the limit state function with minimal distance to the origin of the Standard Normal space. As such, it is the most appropriate point to linearize the limit state function. For each limit state function, the gradient vector is evaluated as (Equation 8):

$$\boldsymbol{\nabla}_{g_i} = \left\{\frac{dg_i}{dy_m}\right\}_{m=1,\dots,n_{RV}} \tag{8}$$

In Equation 6, vector $\boldsymbol{\alpha}_i$ is the normalized gradient of the i^{th} constraint, also known as direction cosine (Equation 9):

$$\boldsymbol{\alpha}_i = \frac{\boldsymbol{\nabla}_{g_i}}{\left\|\boldsymbol{\nabla}_{g_i}\right\|} = \{\alpha_m\}_{m=1,\dots,n_{RV}} \tag{9}$$

The squared normalized direction cosines α_m^2 inform about the contribution of each random variable to the calculated failure probabilities, since (Equation 10):

$$\sum_m \alpha_m^2 = 1 \tag{10}$$

The formulation in Equations 5 and 6 is a generalization of the original formulation in [33], which addresses non-Gaussian and correlated variables. SLA does not search for the design point of each constraint at each iteration. Instead, an approximation of the design point of active constraints is obtained by solving the KKT conditions. An implicit assumption in SLA is that the sequence of design point approximations converges to the true design point.

If a limit state function is highly non-linear in the reduced variable space or if there are multiple design points for a given limit state, then SLA may not converge to the global optimum. Such issues are well-known in FORM and related methods.

The SLA algorithm starts with initial choices for $\mathbf{d}_0$ and $\mathbf{x}_{i0}$ (e.g., $\mathbf{x}_{i0} = \mu_{\mathbf{X}}$), for $k = 0$, and by evaluating the objective function and constraints in Equation 6. Point $\mathbf{d}_{k+1}$ is evaluated using an appropriate optimization algorithm, counter k is updated ($k = k + 1$), and transformation matrices $\left(\mathbf{J}_{xy}\right)_k$ and normalized gradient vectors $\boldsymbol{\alpha}_{i0}$, $i = 1, \dots, n_{LS}$ are updated. At this point, the design point estimates can be updated, making $\mathbf{x}_{ik} = (\mu_{\mathbf{X}})_k - \left(\mathbf{J}_{xy}\right)_{ik} \boldsymbol{\alpha}_{ik} \beta_{Ti}$. During the interactive procedure, the algorithm first checks if $(\mu_{\mathbf{X}})_k$ has changed from the last iteration. In a positive case, the $\boldsymbol{\alpha}_{ik}$ vectors are updated. If not, the same gradient vector $\boldsymbol{\alpha}_{ik}$ is used to calculate $\mathbf{x}_{ik} = (\mu_{\mathbf{X}})_k - \left(\mathbf{J}_{xy}\right)_{ik} \boldsymbol{\alpha}_{ik} \beta_{Ti}$. This step is essential to keep vectors $(\mu_{\mathbf{X}})_k$, and $\mathbf{x}_{ik}$ consistent, but it also increases the efficiency of the algorithm [18]–[20].

2.4 Optimization algorithm

The numerical procedure adopted to minimize the objective function is the NLPSolve subroutine of the MAPLE 2019 [58], [59] software. The NLPSolve command solves a nonlinear program (NLP), which involves computing the minimum (or maximum) of a real-valued objective function, possibly subject to constraints. Within the NLPSolve subroutine, the Sequential Quadratic Programming (SQP) method was selected to solve the optimization problem. Numerical derivatives are computed automatically throughout iterations.

2.5 Target reliability index (β_T) for dams

The target reliability indices (β_T) guide the expected performance of the dam. If the dam meets $\beta_T \geq 3$ (high performance) for all failure modes, the expected performance will be good. Dams with a $\beta_T < 3$ (low performance) will be expected to perform poorly and present major rehabilitation problems. A dam with $\beta_T < 1$ very low performance) is classified as hazardous with serious structural problems. The U.S. Army Corps of Engineers [21] gives a guide of β_T values, as shown in Table 1, which is generally used.

Table 1. Target reliability indexes for dam stability analysis [21].

Expected performance level	Reliability index (β)	Probability of failure (P_f)
High	5.0	3.0×10^{-7}
Good	4.0	3.0×10^{-5}
Above average	3.0	1.0×10^{-3}
Below average	2.5	6.0×10^{-3}
Poor	2.0	2.3×10^{-2}
Unsatisfactory	1.5	0.07
Hazardous	1.0	0.16

3 THE APPLICATION PROBLEM

A concrete dam is adopted to illustrate the application of RBDO using the SLA algorithm. We here adopt a section of a concrete dam that satisfies all the deterministic design requirements. The concrete dam has a height of 50 m, and width of 7 m at the crest (a two-way highway exists at the crest). The upstream face is vertical, and the downstream face has an initial slope of 1V:0.733H. A drainage gallery with a square dimension of 2.0 m is located 5.0 m from the upstream face to reduce uplift forces in the dam foundation and body of the dam. The spillway gives a restriction of the maximum water level in the reservoir, and this defines the freeboard, which is 2.0 m under the crest of the dam. The bedrock, foundation of the dam, is considered waterproof and impenetrable.

The downstream face slope is often considered the design variable. To meet stability requirements, the slope is usually in the order of 1V:0.7H to 1V:0.8H, depending upon uplift assumptions [60]. However, for higher dams with low-density concrete or under seismic loading, this relationship will be higher to meet stability requirements [61].

Some recommendations in the literature of minimal distances between the drainage gallery and the upstream wall face of the dam were found. USACE [4] and USBR [7] recommend a minimum distance of 1.524 m (5 ft.) for the placement of concrete mass and to reduce stress concentrations. USACE [3] suggest a higher distance than 5 % of the water reservoir height to have a reduction of the uplift pressure by the gallery drainage. The upstream face of the gallery shall be located at a minimum distance of 5 % of the maximum reservoir head or 3 m from the upstream face, whichever is greater [62]. The gallery drainage should be located between 3 m to 9 m away from the upstream face to reduce uplift pressures [63]. To minimize the possibility of cracking with serious leakage from the water reservoir, Jansen [64] states that the gallery must be at least 3 m away from the upstream face and at a distance of at least 5 % of the water reservoir height. El-razek and Elela [65] experimentally found the optimum position of the drainage gallery, a relationship between the horizontal distance of the gallery/Base of the dam gives 0.5. The research by Chawla et al. [66] showed that the size, location, and spacing of the drains impact the distribution of internal uplift pressure by using an analytical solution based on the seepage theory. Later, other authors [67]–[70] demonstrated it numerically with different computational models.

The initial dimensions of the concrete dam follow different suggestions of specialized standard agencies [3]–[6]. There are extensive explanations as to how to define a cross-section of a dam in the literature, but this paper aims to optimize a section and not to explain how to design this section in a deterministic approach. Therefore, all the initial input geometric information of the application problem is defined by: $L_1 = 7$, $L_2 = 40$, $L_3 = 5$, $H_1 = 50$, $H_2 = 5$, $H_3 = 4$, $H_4 = 48$, $H_5 = 3$, and $H_6 = 5$ which is represented in Figure 2(a). All the dimensions are in meters.

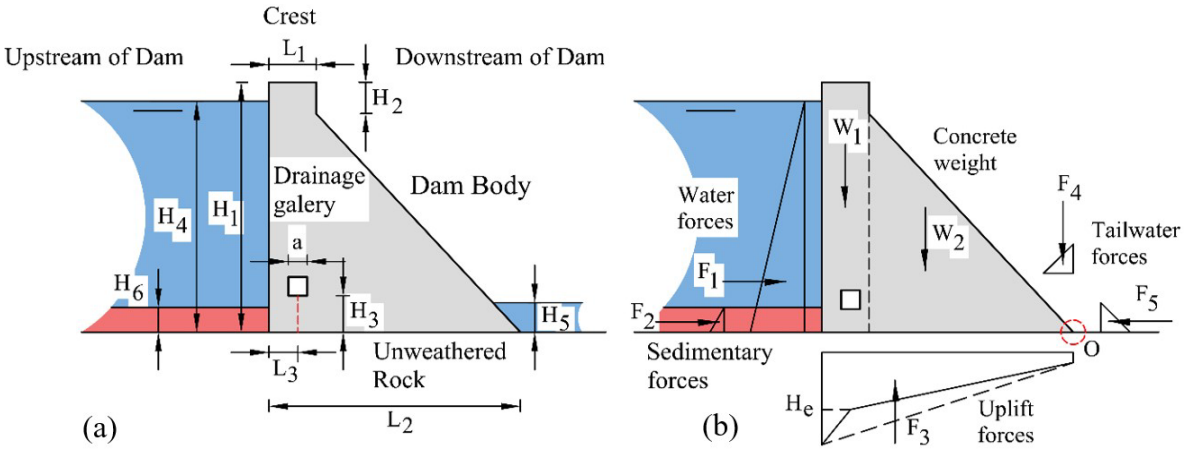

Figure 2. Reliability-based design optimization of a concrete dam: (a) geometry and (b) forces involved in stability analysis.

In the design of concrete dams, different safety factors are used for different loading conditions (e.g., normal, accidental, reservoir empty, earthquake, …, etc.); this study considers only the normal loading condition. Yet, for a single loading condition, different failure modes must be considered. The methodology presented herein can be employed with different loading conditions, given additional loads.

The uplift pressure acting on a concrete dam foundation is a function of the drainage system. If there is no drainage system at the dam foundation, the upstream and downstream uplift pressures are equivalent to the respective water columns in the upstream and downstream reservoirs of the dam. For dams with a drainage system, the effectiveness of the drainage system will depend on depth, size, geology conditions and spacing of the drains; the characteristics of the foundation; and the facility with which the drains can be maintained [3]. The hydraulic efficiency (E) or the hydraulic inefficiency ($k_{DG} = 1 - E$) of the drain system is used to estimate the uplift pressures. The USBR [7] suggests a maximum $E = 66$ % for new dams; ELETROBRÁS [5] suggests a $k_{DG} = 0.33$ and the USACE [4] limits a maximum of $E = 50$ %. French guidelines [8] recommend values of E between 67 % to 50 % for regular geology and less for unfavorable geology. The Chinese design guideline [71] suggests an E between 60 % to 80 %.

In this study, the theoretical approach of ELETROBRÁS [5] and USBR [7] was taken into account to determine the uplift pressure in the drainage line. The equivalent water column height is (Equations 11 and 12):

$$H_e = k_{DG}(H_4 - H_5) + H_5 \text{ for } H_5 > H_3 \tag{11}$$

$$H_e = k_{DG}(H_4 - H_3) + H_3 \text{ for } H_3 > H_5 \quad (12)$$

The forces and moment arms involved in the overturning limit state are listed in Table 2 and shown in Figure 2(b).

The mean value (μ) and coefficient of variation (COV) of the problems random variables are obtained from related studies in the literature, as shown in Table 3. The uncertain parameters involved in the analysis are the specific weight of the concrete (γ_c), the ultimate bearing capacity of rock mass foundation (q_u), the specific weight of the sedimentary material (γ_s), the friction angle of the sedimentary material (ϕ'_s), the cohesion along the interface between dam base and foundation rock (c'_{rc}), the friction angle along the interface between the dam base and foundation rock (ϕ'_{rc}) and the coefficient of drainage gallery inefficiency (k_{DG}). Although the specific weight of the water (γ_w) has a statistical variation as function of temperature, gravity acceleration is employed as a constant value, equal to 9.81 kN/m^3 [3], [4], [72]. The uncertain parameters are assumed to have normal (N) distributions, following Table 3. No correlation is considered between random parameters; hence, the correlation matrix is the identity matrix.

Table 2. Forces and moment arms for the rotational failure of the concrete dam.

Force	Moment arm
$W_1 = L_1 H_1 \gamma_c$	$a_1 = L_2 - \frac{L_1}{2}$
$W_2 = \frac{(L_2 - L_1)(H_1 - H_2)}{2}\gamma_c$	$a_2 = \frac{2(L_2 - L_1)}{3}$
$W_3 = a^2 \gamma_c$	$a_3 = L_2 - L_3$
$F_1 = \frac{H_4^2}{2}\gamma_w$	$a_{F1} = \frac{H_4}{3}$
$F_2 = \frac{H_6^2(1 - \sin\phi'_s)}{2}\gamma_s$	$a_{F2} = \frac{H_6}{3}$
$F_3 = \frac{H_4 L_3 + H_e L_2 + H_5 L_2 - H_5 L_3}{2}\gamma_w$	$a_{F3} = \frac{2\left[H_4\left(\frac{L_3 L_2}{2} - \frac{L_3^2}{6}\right) + H_e\left(\frac{L_2^2}{3} - \frac{L_3 L_2}{6}\right) + H_5\left(\frac{L_2^2}{6} + \frac{L_3^2}{6} - \frac{L_3 L_2}{3}\right)\right]}{H_4 L_3 + H_e L_2 + H_5(L_2 - L_3)}$
$F_4 = \frac{H_5^2(L_2 - L_1)}{2(H_1 - H_2)}\gamma_w$	$a_{F4} = \frac{H_5(L_2 - L_1)}{3(H_1 - H_2)}$
$F_5 = \frac{H_5^2}{2}\gamma_w$	$a_{F5} = \frac{H_5}{3}$

Table 3. Input parameters of the application problem.

Analysis	Parameters	μ	COV (%)	Observation
Concrete	γ_c (kN/m^3)	24	4	[1]
Rock	q_u (MPa)	15	50	[2]
Sedimentary material	γ_s (kN/m^3)	19	7	[3]
	$\phi's$ (kN/m^3)	28	20	[4]
Interface Rock-Concrete	c'_{rc} (kPa)	250	40	[5]
	ϕ'_{rc} (kN/m^3)	35	30	[6]
Drainage gallery inefficiency	k_{DG}	0.33	20	[7]

Observation [1]: The COV of γ_C is 4 % [73] and other authors have related a COV about 3 % to 5 % [74]. Nominal values were based on CFBR [8] and JCSS [73]. [2]: The COV of q_u for a rock foundation varies from 25.9 % to 44.5 % [75], 127 % [76], and for soil foundations, 20 % [11]. Nominal values for a sandstone rock was taken from Duncan [77]. [3]: The COV of γ_S for all the different soils varies from 3 % to 11 % [78], [79]. Nominal values were based on Fredlund et al. [80] and USBR [81]. [4]: The COV of ϕ' for all the different soils varies from 10 % to 30 % in clays [78], [79]. Nominal values were taken from Fredlund et al. [80] and USBR [81]. [5]: The COV of c'_{rc} for all the different rocks varies from 36 % to 40 % [2], 64 % to 69 % [82], 65 % [83] and 44 % [84]. Nominal values were based on Pires et al. [74]. [6]: The COV of ϕ'_{RC} for all the different rocks varies from 25 % to 30 % [2], 15 % [84], and 40 % [83]. Nominal values were taken from NAVFAC DM7-02 [85]. [7]: The COV of k in a concrete dam varies from 15 % to 30 % [74]. Nominal values were based on FERC [6] and USACE [3].

The design of a concrete dam is based on the stability analysis of the cross-section, considering all possible rigid body mechanisms. Although stresses shall not exceed some admissible limits, the safety of concrete gravity dams is

independent of the mechanical strength of the concrete, since different mechanics of failures (e.g. sliding, overturning, …, etc.) occur before a conditioning stress field is achieved [86].

The following five failure modes are determined for the present study: (a) overturning failure, (b) sliding failure, (c) flotation failure, (d) eccentricity failure, and (e) bearing capacity failure. For the initial design, recommended safety factors were taken from the Chinese standards [1], [2], U.S. Army Corps of Engineers [3], [4], Brazilian Power Plants – ELETROBRÁS [5], Federal Energy Regulatory Commission [6], United States Bureau of Reclamation [7] and others [9], [10].

In the sequence, these five failure modes (*a* to *e*) are described.

(*a*) The factor of safety for overturning failure (FS_O) is given by a relationship between resisting moment (M_R) and overturning moment (M_A) (Equation 13):

$$FS_O = \frac{\sum M_R}{\sum M_A} = \frac{W_1 a_1 + W_2 a_2 - W_3 a_3 + F_4 a_{F4} + F_5 a_{F5}}{F_1 a_{F1} + F_2 a_{F2} + F_3 a_{F3}} \geq 2.0 \tag{13}$$

(*b*) The factor of safety for sliding failure (FS_S) is given by a relationship between resisting forces (F_R) and resultant horizontal forces (F_O) (Equation 14):

$$FS_S = \frac{F_R}{F_O} = \frac{N \tan \phi'_{rc} + c'_{rc} A}{F_O} = \frac{(W_1 + W_2 - W_3 - F_3 + F_4) \tan \phi'_{rc} + c'_{rc} L_2}{F_1 + F_2 - F_5} \geq 2.0 \tag{14}$$

where *N* is the sum of normal forces and *A* is the area of contact on the plane under analysis.

(*c*) The factor of safety for flotation failure (FS_F) is given by a relationship between gravitational forces (F_V) and resultant uplift pressure forces (F_U) (Equation 15):

$$FS_F = \frac{F_V}{F_U} = \frac{W_1 + W_2 - W_3 + F_4}{F_3} \geq 1.3 \tag{15}$$

(*d*) The eccentricity factor of safety (FS_E) is given by a relationship between the base of the dam (L_2) and six times its eccentricity (e) (Equation 16):

$$FS_E = \frac{L_2}{6e} \geq 1 \tag{16}$$

(*e*) The factor of safety of bearing capacity failure (FS_B) is given by a relationship between the ultimate bearing capacity (q_u) and maximum foundation pressure (q_{max}) (Equation 17):

$$FS_B = \frac{q_u}{q_{max}} = \frac{q_u}{\frac{F_V}{L_2}\left(1 + \frac{6 * e}{L_2}\right)} \geq 3 \tag{17}$$

where *e* is the eccentricity of the resultant forces, defined as (Equation 18):

$$e = \frac{L_2}{2} - X = \frac{L_2}{2} - \frac{\sum M_R - \sum M_A}{F_V} \tag{18}$$

where *X* is the arm of the resultant net forces.

Using the initial geometry input, forces and arm moments involved in the safety analysis (Figure 1 and Table 1), the following factors of safety are determined: (a) $FS_O = 2.15$, (b) $FS_S = 2.17$, (c) $FS_F = 4.91$, (d) $FS_E = 1.16$ and (e) $FS_B = 8.20$. All the factors of safety evaluated herein in the mean value (deterministic) analysis satisfy the minimum stability criterion.

The downstream face slope defines the final volume of the concrete dam. If the base of the dam is increased, the safety factors increase, but this also has an impact on construction cost. The position of the drainage gallery

defines the uplift forces, and it is an important part of the determination of the FSs. The uplift forces increase about 5% for every meter the drainage gallery is moved away from the upstream face. It affects the determination of the FSs with a reduction of about 4% in flotation and eccentricity failure, 2% in overturning and bearing capacity failure, and 1% in sliding failure. If the gallery drainage is defined away of the upstream face, the base of the dam should be increased to meet all FSs.

4 IMPLEMENTATION DETAILS OF OPTIMIZATION PROBLEM

4.1 Optimization modeling using the SLA method

To maximize the performance of the structure, or to minimize the concrete volume (cost of the geotechnical structure), reliability-based optimization of the case-study dam is considered herein. The SLA method is employed, where optimal design and target reliability are obtained simultaneously in the same optimization loop. This section presents an overview of the SLA method for a geotechnical problem. The following procedure is illustrated by the flowchart in Figure 3:

Step (1): All the input data of a geotechnical problem are defined in this step. The input data are defined by the initial dimension of the structure, safety level or target reliability index for every failure mode (β_{Ti}), design variables $\mathbf{d}$, properties variables $\mathbf{X}$, upper (ub), and lower (lb) bound vectors for all deterministic and probabilistic design variables. The variables can be represented by the mean value (μ) and standard deviation (σ) or the coefficient of variation (COV= σ/ μ) in a Normal distribution (N) or Lognormal distribution (LN).

Step (2): For the initial design, the mean values of random variables are used.

Step (3): Calculate normalized gradient vector ($\boldsymbol{\alpha}_{i0}$).

Step (4): Calculate $f(\mathbf{d}_{dk}, \mu_{\mathrm{X}})$.

Step (5): The unique loop begins with k= 0, and runs until a convergence criterion is met.

Step (6): Calculate the normalized gradient vector ($\boldsymbol{\alpha}_{ik}$).

Step (7): Calculate $\mathbf{d}_{ik}$ and $\mathbf{x}_{ik}$ using the new values of μ_{dk} and μ_{Xk}. The point of minimum performance is linearly approximated at each iteration. If the variables have non-normal distributions, it is necessary to transform them into equivalent normal distributions. The two conditions involved in this transformation require that the cumulative distribution function (CDF) and the probability density function (PDF) of non-normal variables and equivalent normal variables to be equal at the current point of minimum performance.

Step (8): Calculate $g_i(\mathbf{d}_{ik}, \mathbf{x}_{ik})$.

Step (9): Minimize f using NLPSolve in MAPLE. As a result, this minimization results in new values in μ_{d} and μ_{X}. In this work, the Sequential Quadratic Programming (SQP) is used. SQP is one of the most successful methods for the numerical solution of constrained nonlinear optimization problems. It relies on a solid theoretical foundation and provides powerful algorithmic tools for solving large-scale technologically relevant problems. SQP is already available in most computer algebra software.

Step (10): An optimization condition is used to finish the optimization. The designer defines the tolerance of the analysis (TOL).

Step (11): The results of the optimization analysis (number of evaluations, sensitivity coefficients at DP, optimized structure, reliability index, and the probability of failure for every limit state function, evaluation time, DP, etc.) are shown in the OUTPUT.txt file.

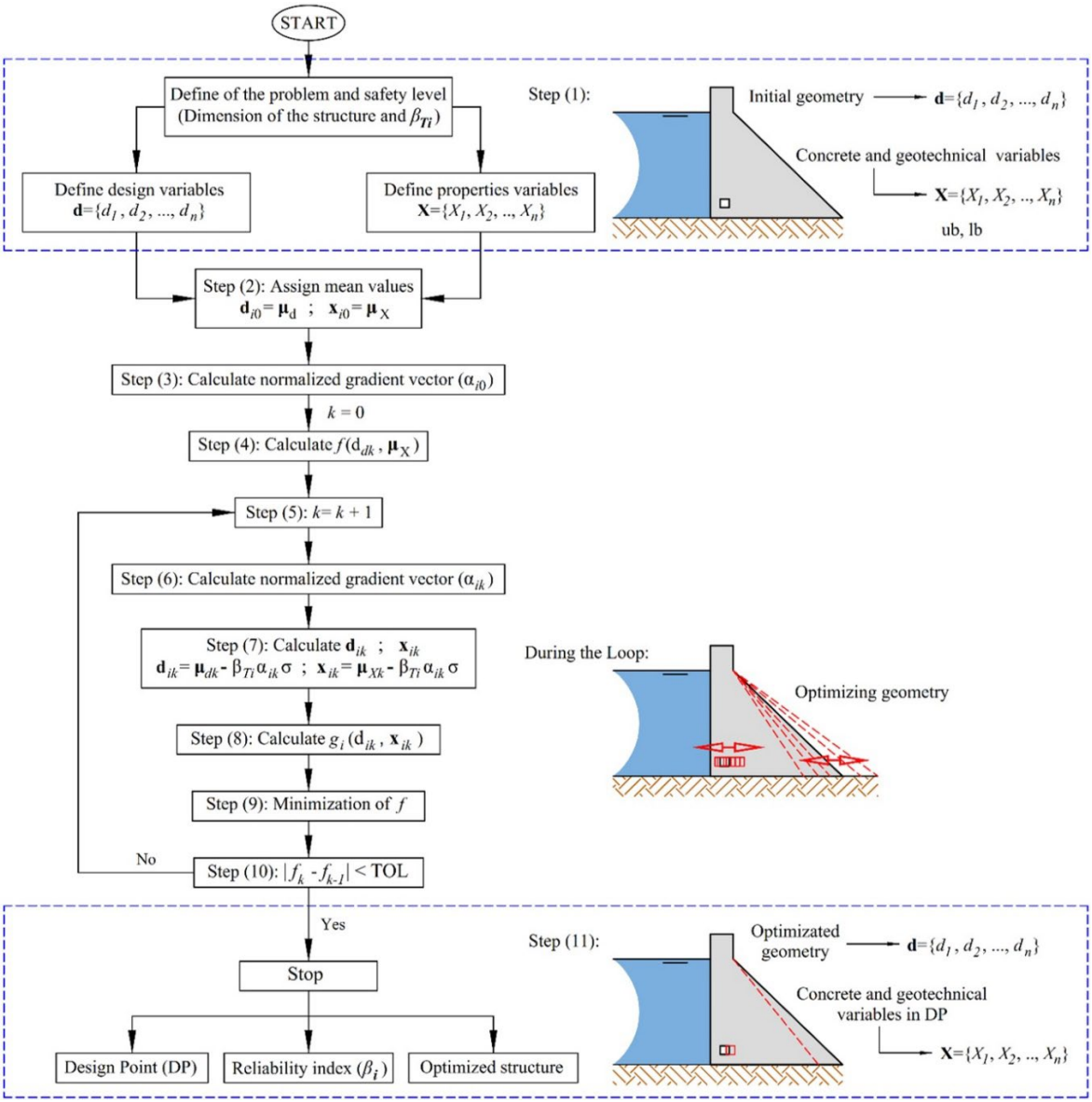

Figure 3. Flowchart of SLA algorithm for a geotechnical problem (based on [33]).

4.2 Definition of limit state functions and procedure for design optimization

The mean objective is to minimize the cross-section area of the dam, and to find the best position of the gallery drainage by changing the design variables $\mathbf{d} = \{L_2, L_3\}$. In this study, initially the target reliability index is $\beta_T = 3.0$ for all failure modes, which corresponds to a probability of failure $P_{fT} \geq 1.0\text{x}10^{-3}$. Considering target reliability indexes suggested in [21], the expected performance level of the design dam will be "*above average*". The design space to meet these objectives is $0.7 * H_1 \leq L_2 \leq 2 * H_1$ m; $0.05 * H_4 \leq L_3 \leq 15$ m; or $3.0 \leq L_3 \leq 15$ m. The reliability-based design optimization (RBDO) problem can be written as (Equation 19):

Find $\mathbf{d}^*$ which minimizes $f(\mathbf{d}) = L_1H_1 + 0.5(L_2 - L_1)(H_1 - H_2) - a^2$

Subject to: $\beta_i(\mathbf{d}) \geq \beta_T, i = 1, 2, 3, 4; \mathbf{d} \in S$ (19)

where $f(\mathbf{d})$ is the cross-section area of the concrete dam and $\beta_1, \beta_2, \beta_3,$ and β_4 are the reliability constraints for the limit states of (a) overturning, (b) sliding, (c) flotation, and (d) eccentricity, respectively. These reliability constraints are evaluated considering the following limit state functions.

(a) The limit state function for overturning, with respect to the most extreme downstream point of the surface under analysis, is defined as (Equation 20):

$$g_O(\boldsymbol{x}) = \sum M_R - \sum M_A \tag{20}$$

(b) The limit state function for sliding along the surface under analysis is defined by (Equation 21):

$$g_S(\boldsymbol{x}) = F_R - F_O \tag{21}$$

(c) The limit state function for flotation is defined by (Equation 22):

$$g_F(\boldsymbol{x}) = F_V - F_U \tag{22}$$

(d) The limit state function for eccentricity is defined as (Equation 23):

$$g_E(\boldsymbol{x}) = 1 - \frac{6e}{L_2} \tag{23}$$

Limit state functions for overturning (Equation 20), sliding (Equation 21), flotation (Equation 22), and eccentricity (Equation 23) are the geotechnical design requirements. The limit state function for bearing capacity failure was not considered because of the high value of the safety factor.

5 OPTIMIZATION ANALYSIS AND RESULTS

RBDO analyses were performed for the same scenario described in the mean value (deterministic) analysis, including four different failure modes. A Single-Loop Approach (SLA) was implemented in the MAPLE 2019 software, as described in Sections 2 and 3. In this study, a common desktop computer was used, with a processor speed of 2.1 GHz (2 processors) and 64-GB RAM memory. The average computational time for each analysis is less than 100 min.

The RBDO analysis considered 6 random variables of the problem (γ_c, γ_s, ϕ'_s, c'_{rc}, $\phi'_{rc,}$ and k_{DG}), as shown in Table 3. The following optimization analysis results are presented:

Initial results;
RBDO for different target reliabilities (β_T);
Sensitivity of failure probabilities do random variables;
RBDO for different dam heights;
Comparison of RBDO with DDO.

5.1 Initial results

Starting from an initial design of $\mathbf{d} = \{L_2, L_3\} = \{40, 5\}$, an initial optimum design is found by solving the optimization problem in Equation 19. An optimal design of $\mathbf{d} = \{L_2, L_3\} = \{77.4, 3.0\}$ is found for $\beta_T = 3.0$ and height of the dam H_1= 50 m. In initial RBDO result with the SLA method, the limit state function for sliding along the surface $\big(g_S(\boldsymbol{x})\big)$ controls the optimal response, meaning that $g_S(\boldsymbol{x})$ is the active constraint at the optimal point. In this solution, constraints g_O, g_F and g_E are not active.

The initial downstream face has a slope of 1V:0.733H, and the final slope optimized is 1V:1.56H for $\beta_T = 3.0$. In terms of area, the areas of the initial design and global optimal design are 1088.5 m^2 and 1929.74 m^2. The difference in areas between both approaches is 43.59 % higher for the RBDO approach. The drainage system is moved from 5 m, in the deterministic design, to 3 m in the RBDO design, with reference to dam upstream. It means less uplift pressure acting on the concrete dam foundation.

All the design points in the above solutions were found using the SLA algorithm. None of the limit state functions was excessively nonlinear; hence, no convergence problems were observed in the analyses. In the case of nonlinear limit state functions, other algorithms based on Monte Carlo simulation may be required (see, for instance, the discussion in Rashki et al. [87], [88]). The algorithm was validated with earlier studies [33], [34]. The difference of results was less than 1 % between the results reported by [33], [34] and the present algorithm developed in MAPLE 2019.

5.2 RBDO for different β_T

In this section, the target reliability index (β_T) is changed to analyze the variation in the area between the original design and optimal design. From the results in Figure 4 and Table 4, we concluded that for the dam studied herein, the results are proportional, meaning smaller reliability indices defined smaller areas. In the case of smaller areas, such as $\beta_T = 1.5$ to 2.0, the area is very similar to the deterministic analysis. In a conventional design, the deterministic area is used, and it means an Unsatisfactory ($\beta_T = 1.5$) to Poor ($\beta_T = 2.0$) expected performance level according to Table 1 (USACE [21]). A considerable difference is found between $\beta_T = 1.5$ to 3.0 with more than 43 % in terms of concrete area. Sometimes, this increase of concrete area is deemed unnecessary by geotechnical engineers. Deterministic analyses are performed with the optimized section where large *FSs* are found. In function of the deterministic and RBDO results, the designer and owner or investor choose the final section assuming an acceptable performance level of the dam.

Computationally, values of lengths of the dam for different β_T can be obtained. Using larger values of β_T (2.5, 3.0, or more), the design of the dam will be unrealistic in terms of benefit/cost, but it will have a guaranteed performance level.

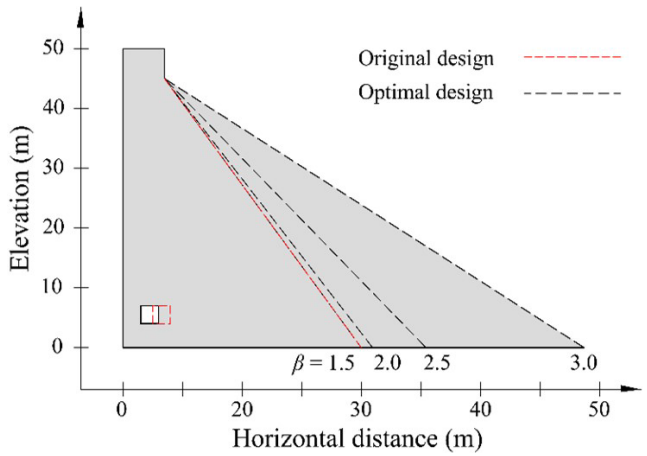

Figure 4. Comparison of the initial design and the optimal designs obtained with RBDO.

Table 4. Results of the RBDO reliability analysis.

Description	β_T	L_2	L_3	Cross-section Area	Difference (%)
Initial design	-	40.0	5.0	1088.50	
Optimal design	1.5	40.3	3.0	1095.60	0.65
	2	41.9	3.0	1131.16	3.77
	2.5	50.9	3.0	1332.94	18.34
	3	77.4	3.0	1929.74	43.59

In Table 5, values of the four limit state functions are presented at their design points ($g_i(\mathbf{x}_i^*)$), at the end of the optimization. A value close to zero indicates an active constraint, meaning that the corresponding failure mode controlled the optimum design (i.e., halted the objective function from being further minimized). As observed in Table 5, for the studied dam the overturning (g_O) and flotation (g_F) failure modes never become active, for any of the target reliabilities considered herein. The eccentricity (g_E) failure mode is the active constraint for the RBDO solution for smaller reliabilities ($\beta_T = 1.5$ and 2.0), and the sliding failure mode (g_S) is the active constraint for large β_T ($\beta_T = 2.5$ and 3.0).

Table 5. Limit state function values at the corresponding design points for different target reliability index.

Failure mode	Target reliability			
	$\beta_T = 1.5$	$\beta_T = 2.0$	$\beta_T = 2.5$	$\beta_T = 3.0$
Overturning (g_O)	306752.73	313218.48	485929.04	1196889.79
Sliding (g_S)	3842.72	1244.79	**-5.97 x10^{-13}**	**-8.53 x10^{-13}**
Flotation (g_F)	19236.12	19121.93	21595.01	29776.17
Eccentricity (g_E)	**-5.21 x10^{-13}**	**5.55 x10^{-16}**	0.27	0.64

5.3 Sensitivity of variables

By using the SLA method, a sensitivity analysis through the direction cosines (α^2) at the design points is conducted, revealing the most significant variables for each failure mode. Figure 5 shows the sensitivity coefficients α^2 of each random variable, for the four limit state functions and for different target reliabilities β_T. The sensitivity coefficients for the distance of drainage gallery (L_3), specific weight of the sedimentary material (γ_s) and friction angle of the sedimentary material (ϕ'_s) do not appear in Figure 5 because they are nearly zero ($\alpha^2 \approx 0$) for all failure modes; hence, these random variables have negligible contributions to the computed failure probabilities and can be considered deterministic.

As observed in Figure 5, the cohesion and friction angle along dam base interface with foundation rock (variables c'_{rc} and ϕ'_{rc}) have a considerable contribution for the sliding failure mode, and variables L_2, γ_c, and k_{DG} are important in overturning, flotation, and eccentricity failure modes. The drainage gallery inefficiency (k_{DG}) increases in importance when β_T increases.

Since for large β_T failure is controlled by sliding, it turns out that variables c'_{rc} and ϕ'_{rc} also control design for large β_T. In a similar way, variables L_2, γ_c, and k_{DG} control the optimal design for small β_T.

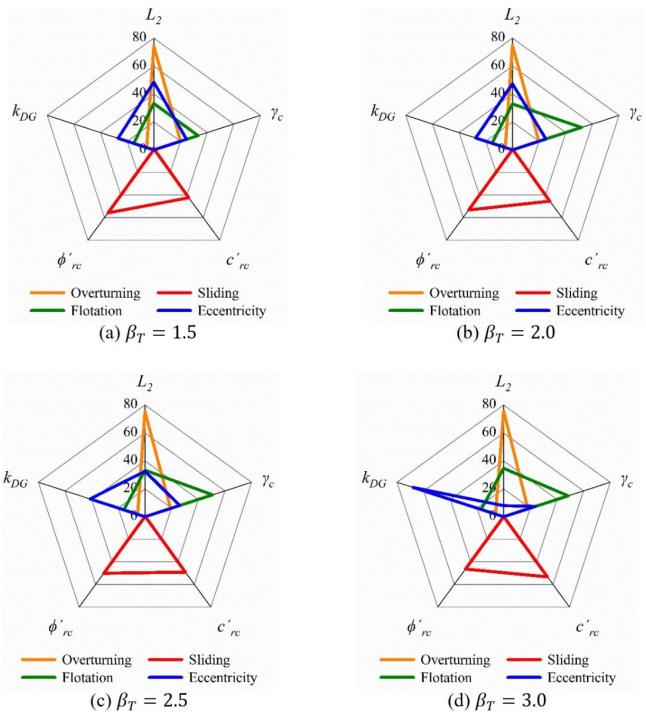

Figure 5. Sensitivity coefficients for different failure modes and target reliability indexes (β_T).

5.4 RBDO for different dam heights

In this section, we address the optimization of dams of different heights, with same normal load condition as defined in Section 3. Dam heights of $H_1 = 30, 40, 50, 60$ and 70 m are considered in this section.

Optimization results are shown in Figure 6, for different dam heights. As can be observed in this figure, there is a range of β_T values for which the objective function (dam cross-section area) and optimum dam base L_2 do not change much with the target reliability β_T. Within this "flat" region of the graphs in Figure 6, the change in area and in dam base is smaller than 10% (for same dam height H_1), and the optimum design is controlled by the eccentricity failure mode. Within the "non-flat" region, optimum dam design is controlled by the sliding failure mode, and optimum area and dam base change more as a function of β_T. For a dam with height (H_1) of 70 m, for instance, optimum dam base L_2 is almost the same for β_T between 1.5 and 1.9; but changes significantly as a function of β_T for $\beta_T > 2$.

As noted in Section 5.2, this relative importance of failure modes, changing with β_T and dam heigth, could be different in a deterministic optimization. To investigate this claim, a comparative study is performed in the sequence, comparing results of RBDO and DDO.

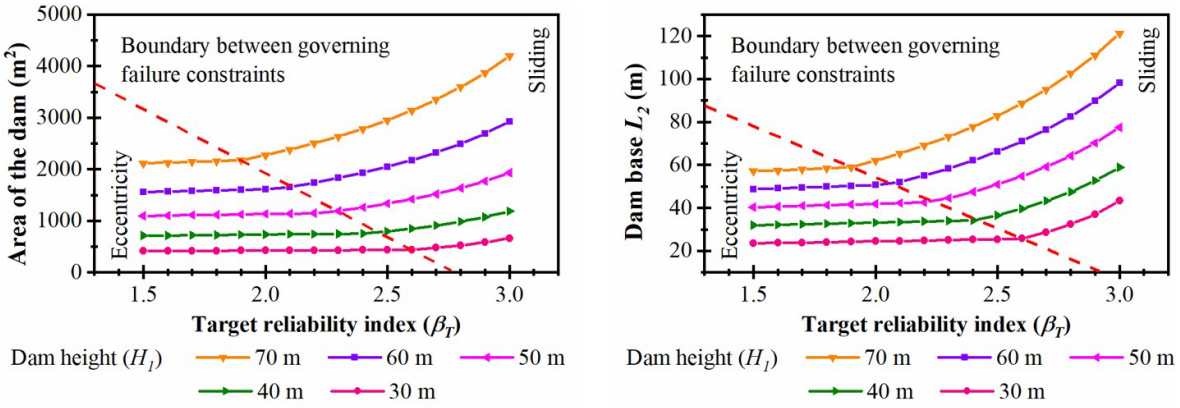

(a) in terms of total area of concrete. (b) in terms of dam base (L_2).

Figure 6. Optimal RBDO solutions for different dam heights.

5.5 Comparison of RBDO with DDO

It is well reported in the literature on reliability of geotechnical soil structures [79], [89] that the most probable slip surface, or the slip surface corresponding to the design point $\mathbf{x}_i^*$, is different than the slip surface corresponding to the minimum factor of safety. This has been demonstrated, for instance, in a study addressing reliability of earth dams [79]. Similarly, in a study addressing rapid drawdown of earth dams [78], it was shown that the critical time obtained in a probabilistic analysis is not the same as that obtained in a deterministic design. Making a parallel of these results, with results presented in this paper, it is perfectly plausible that a deterministic optimization could result in different controlling failure modes, in comparison to those shown in Table 5.

Results of a deterministic design optimization (DDO) depend on the safety factors employed as constraints, in the same way as results of Reliability-based Design Optimization (RBDO) depend on the target reliabilities used as constraints in Equation 5. To make a "fair" comparison between the approaches, it is reasonable to solve the RBDO problem first, and use as constraint in DDO the minimum safety factor found in RBDO (Beck and Gomes, 2012). Results are computed herein for dam heights $H_1 = 70$ and 30 m, and different β_T. The considered β_T values target the boundary between governing failure constraints (Figure 6). RBDO and DDO solutions are computed starting from initial designs $\mathbf{d} = \{L_2, L_3\} = \{60, 5\}$ for $H_1 = 70$, and $\mathbf{d} = \{L_2, L_3\} = \{25.3, 5\}$ for $H_1 = 30$.

Results are compared in Table 6, which shows that the optimum solutions are the same, for all RBDO and DDO problems considered. This is a consequence of the small number of design parameters considered herein (L_2 and L_3). As shown in Beck and Gomes (2012), this is not to be expected in general, since different failure modes control de optimum RBDO and DDO designs, as shown in the sequence.

Table 6 shows the values of the four limit state functions, evaluated at the corresponding design points ($g_i(\mathbf{x}_i^*)$), for the optimum RBDO designs. The minimum values of $g_i(\mathbf{x}_i^*)$, identified in bold face in Table 6, indicate the active reliability constraint for the optimum RBDO design. As can be observed, for $H_1 = 70$ and $\beta_T = 1.8$, eccentricity is the active constraint in RBDO, and leads to the smallest FS. For all other $H_1 = 70$ cases, sliding failure is the active reliability constraint. Yet, the minimum FS is obtained for the eccentricity failure mode, for $\beta_T \leq 2.1$, and for the sliding failure only for $\beta_T = 2.2$. Something similar is noted for $H_1 = 30$, where for $\beta_T = 2.5$ eccentricity is the active

reliability constraint and the minimum SF, but for other β_T values, differences are observed between active reliability constraint and minimal safety factor.

The observation that the active reliability constraint is different to the minimum safety factor constrain depending on problem parameters is evidence that the two formulations are not equivalent. For instance, if the active reliability constrain is chosen as the reference for the safety factor to be respected in DDO, like a design for minimum FS=1,98 for $H_1 = 70$ and $\beta_T = 1.9$, then the optimum solution is found as $L_2 = 65{,}55$ m, quite different to the RBDO optimum of $L_2 = 58.9$ meters.

Table 6. RBDO and DDO results for Limit state functions in the design point for different target reliability index.

H_1	β_T	Analysis	L_2	L_3	Overturning (g_O)	Sliding (g_S)	Flotation (g_F)	Eccentricity (g_E)
70	1.8	RBDO	58.40	3.00	845917.08	869.37	37470.00	**-5.10 x10^{-9}**
		DDO			2.34	1.96	5.75	**1.41**
	1.9	RBDO	58.90	3.00	851773.89	**2.61 x10^{-12}**	37461.54	1.93 x10^{-3}
		DDO			2.37	1.98	5.75	**1.44**
	2	RBDO	61.99	3.00	972406.90	**-3.41 x10^{-12}**	38868.02	9.51 x10^{-2}
		DDO			2.50	2.07	5.74	**1.67**
	2.1	RBDO	65.37	3.00	1109851.24	**-8.53 x10^{-13}**	40404.58	0.18
		DDO			2.65	2.18	5.74	**1.96**
	2.2	RBDO	69.08	3.00	1267534.89	**1.19 x10^{-12}**	42091.45	0.27
		DDO			2.81	**2.29**	5.73	2.35
	2.5	RBDO	25.42	3.00	70483.94	265.11	6955.87	**-2.22 x10^{-16}**
		DDO			2.44	3.15	4.71	**1.51**
	2.6	RBDO	25.76	3.00	71804.29	**-1.42 x10^{-13}**	6968.93	9.81 x10^{-3}
		DDO			2.47	3.18	4.71	**1.56**
	2.7	RBDO	28.72	3.00	93075.74	**4.55 x10^{-13}**	7456.92	0.17
		DDO			2.70	3.50	4.66	**2.03**
	2.8	RBDO	32.39	3.00	121861.48	**8.53 x10^{-14}**	8063.73	0.32
		DDO			2.95	3.89	4.60	**2.78**
	2.9	RBDO	37.07	3.00	162410.96	**-5.68 x10^{-14}**	8838.91	0.444
		DDO			**3.21**	4.38	4.55	4.14

6 CONCLUSIONS

In this study, we addressed the reliability-based design optimization of a concrete dam. This allowed us to find the minimal dam cross area, or minimum dam base, and the optimal location of drainage gallery, by respecting reliability constraints with respect to four failure modes related to overturning, sliding, flotation and eccentricity failure. An efficient mono-level single loop approach was employed to keep the computational cost under control. In all solutions, optimal placement of the drainage gallery changed from 5 m of the upstream to the minimum of 3 m. The active reliability constraint at the end of the optimization reveals the failure mode which controls optimum design. It was shown how the controlling failure mode changes as a function of target reliability index β_T and dam height, and how these do not correspond to the minimum safety factors of deterministic design. For small target reliabilities and lower dam heights, optimal design is controlled by the eccentricity failure mode, and does not change much with β_T. For larger target reliabilities and larger dam heights, optimum design is controlled by sliding and changes significantly with β_T. The analysis also reveals which random variables have the greater contributions to failure probabilities, at the final (optimal) dam configurations. For lower dams and smaller β_T's, optimal design is controlled by eccentricity, and the most relevant uncertain geotechnical parameters are the base length of the dam, the specific weight of concrete, and the coefficient of drainage gallery inefficiency. For higher dams and larger target reliabilities, failure of optimal dams is controlled by sliding, and the most relevant uncertain parameters for dam equilibrium are the cohesion and friction angle along dam base interface with foundation rock.

ACKNOWLEDGEMENTS

The authors thank the financial support by the Coordination for the Improvement of Higher Education Personnel (CAPES) (Grant number nº 88882.145758/2017-01) and the Brazilian National Council of Scientific and Technological Development (CNPq) for funding the research.

CITATIONS

[1] People's Republic of China Industry Standard, *Design specification for earth-rock fill dams, DL5395-2007*. Beijing, China: China Railway Publishing House, 2007.

[2] China Electric Council, *The Standards Compilation of Water Power in China.* Beijing, China: China Electric Power Press, 2000.

[3] U.S. Army Corps of Engineers – USACE, *Evaluation and Comparison of Stability Analysis and Uplift Criteria for Concrete Gravity Dams by Three Federal Agencies.* Washington DC, USA: USACE Engineer Manual, 2000.

[4] U.S. Army Corps of Engineers – USACE, *Gravity Dam Design*. Washington DC, USA: USACE Engineer Manual, 1995.

[5] ELETROBRÁS, *Civil project criteria for hydroelectric plants (in portuguese)*. Brasília, Brasil: CBDB, 2003.

[6] Federal Energy Regulatory Commission – FERC, *Engineering Guidelines for Evaluation of Hydropower Projects* (Gravity Dams, Report No. FERC 0119-2). Washington, DC, USA: Office of Hydropower Licensing, 2016.

[7] United States Bureau of Reclamation – USBR, *Design of Gravity Dams*. Washington, DC, USA: US Government Printing Office, 1976.

[8] CFBR – Comité Français des Barrages et Réservoirs, *Recommendations for Justification of Stability of Gravity Dams.* France: CFBR, 2012.

[9] P. T. Cruz, *100 Brazilian Dams* (in portuguese).. 2 ed. São Paulo, Brasil: Oficina de textos, 2004.

[10] R. Fell, P. MacGregor, D. Stapledon, G. Bell, and M. Foster, *Geotechnical Engineering of Dams*. 2nd Edition. London: CRC Press, 2015.

[11] Z. Mahmood, "Reliability-based optimization of geotechnical design using a constrained optimization technique," *SN Appl. Sci.*, vol. 2, no. 2, 2020, http://dx.doi.org/10.1007/s42452-020-1948-4.

[12] B. D. Youn and K. K. Choi, "A new response surface methodology for reliability-based design optimization," *Comput. Struc.*, vol. 82, no. 2–3, pp. 241–256, Jan 2004, http://dx.doi.org/10.1016/j.compstruc.2003.09.002.

[13] K.-K. Phoon and J. Ching, *Risk and Reliability in Geotechnical Engineering.* London: Taylor and Francis/CRC Press, 2015.

[14] G. B. Baecher and J. T. Christian, *Reliability and Statistics in Geotechnical Engineering.* Michigan: Wiley, 2003.

[15] ICOLD, "*Bulletin 59: Dam safety*," Paris, France: Commission Internationale des Grand Barrages, 1987.

[16] ICOLD, "*Bulletin 130: Risk Assessment in Dam Safety Management*," Paris, France: Commission Internationale des Grand Barrages, 2005.

[17] D. Bowles, L. Anderson, and T. Glover, "The practice of dam safety risk assessment and management: Its roots, its branches and its fruit," in *18th USCOLD Annu. Meeting and Lecture*, 1998, pp. 233–238.

[18] E. M. Melchers and A. T. Beck, *Structural Reliability Analysis and Prediction*. 3rd ed. Chichester, UK: Wiley, 2018.

[19] A. T. Beck, *Reliability and Safety of Structures* (in portuguese). Sao Paulo, Brazil: Elsevier, 2019.

[20] A. T. Beck, *Structural Reliability* (in portuguese). Sao Paulo, Brazil: Department of Structural Engineering, University of São Paulo, 2017.

[21] U.S. Army Corps of Engineers – USACE, *Introduction to Probability and Reliability Methods for Use in Geotechnical Engineering*. Washington, DC, USA: Defense Technical Information Center, 1997.

[22] L. Zhao, F. Yang, Y. Zhang, H. Dan, and W. Liu, "Effects of shear strength reduction strategies on safety factor of homogeneous slope based on a general nonlinear failure criterion," *Comput. Geotech.*, vol. 63, pp. 215–228, Jan 2015, http://dx.doi.org/10.1016/j.compgeo.2014.08.015.

[23] A. T. Beck and W. J. D. S. Gomes, "A comparison of deterministic, reliability-based and risk-based structural optimization under uncertainty," *Probab. Eng. Mech.*, vol. 28, pp. 18–29, Apr 2012, http://dx.doi.org/10.1016/j.probengmech.2011.08.007.

[24] A. Ang and W. Tang, *Probability Concepts in Engineering: Emphasis on Applications to Civil and Environmental Engineering*. 2nd ed. New Delhi, India: Wiley, 2007.

[25] K.-K. Phoon, *Reliability-Based Design in Geotechnical Engineering: Computations and Applications.* New York: Taylor & Francis, 2008.

[26] I.-T. Yang and Y.-H. Hsieh, "Reliability-based design optimization with discrete design variables and non-smooth performance functions: AB-PSO algorithm," *Autom. Construct.*, vol. 20, no. 5, pp. 610–619, Aug 2011, http://dx.doi.org/10.1016/j.autcon.2010.12.003.

[27] Y. Aoues and A. Chateauneuf, "Benchmark study of numerical methods for reliability-based design optimization," *Struct. Multidiscipl. Optim.*, vol. 41, no. 2, pp. 277–294, Mar 2010, http://dx.doi.org/10.1007/s00158-009-0412-2.

[28] I. Enevoldsen and J. D. Sorensen, "Reliability-based optimization in structural engineering," *Struct. Saf.*, vol. 15, no. 3, pp. 169–196, Sep 1994., http://dx.doi.org/10.1016/0167-4730(94)90039-6.

[29] X. Yu, K. K. Choi, and K. H. Chang, "A mixed design approach for probabilistic structural durability," *Struct. Optim.*, vol. 14, no. 2–3, pp. 81–90, Oct 1997, http://dx.doi.org/10.1007/BF01812509.

[30] J. Tu, K. K. Choi, and Y. H. Park, "A new study on reliability-based design optimization," *J. Mech. Des.*, vol. 121, no. 4, pp. 557–564, Dec 1999, http://dx.doi.org/10.1115/1.2829499.

[31] B. D. Youn, K. K. Choi, and Y. H. Park, "Hybrid analysis method for reliability-based design optimization," *J. Mech. Des.*, vol. 125, no. 2, pp. 221–232, Jun 2003, http://dx.doi.org/10.1115/1.1561042.

[32] X. Chen, T. Hasselman, D. Neill, X. Chen, T. Hasselman, and D. Neill, "Reliability based structural design optimization for practical applications," in *38th Structures, Structural Dynamics, and Mater. Conf.* 1997, vol. 4, no. 1, pp. 2724–2732, http://dx.doi.org/10.2514/6.1997-1403.

[33] J. Liang, Z. P. Mourelatos, and J. Tu, "A single-loop method for reliability-based design optimization," in *30th Design Automation Conf.* 2004, vol. 5, no. 1/2, pp. 419–430, http://dx.doi.org/10.1115/DETC2004-57255.

[34] J. Liang, Z. P. Mourelatos, and E. Nikolaidis, "A single-loop approach for system reliability-based design optimization," *J. Mech. Des.*, vol. 129, no. 12, pp. 1215, 2007, http://dx.doi.org/10.1115/1.2779884.

[35] I. Kaymaz and K. Marti, "Reliability-based design optimization for elastoplastic mechanical structures," *Comput. Struc.*, vol. 85, no. 10, pp. 615–625, May 2007, http://dx.doi.org/10.1016/j.compstruc.2006.08.076.

[36] S. Shan and G. G. Wang, "Reliable design space and complete single-loop reliability-based design optimization," *Reliab. Eng. Syst. Saf.*, vol. 93, no. 8, pp. 1218–1230, 2008, http://dx.doi.org/10.1016/j.ress.2007.07.006.

[37] T. Torng and R. Yang "An advanced reliability based optimization method for robust structural system design," in *34th Structures, Structural Dynamics and Materials Conf.*, 1993, no. 2, pp. 1198–1206, http://dx.doi.org/10.2514/6.1993-1443.

[38] X. Du and W. Chen, "Sequential optimization and reliability assessment method for efficient probabilistic design," *J. Mech. Des.*, vol. 126, no. 2, pp. 225–233, Mar 2004, http://dx.doi.org/10.1115/1.1649968.

[39] G. Cheng, L. Xu, and L. Jiang, "A sequential approximate programming strategy for reliability-based structural optimization," *Comput. Struc.*, vol. 84, no. 21, pp. 1353–1367, Aug 2006, http://dx.doi.org/10.1016/j.compstruc.2006.03.006.

[40] P. Yi, G. Cheng, and L. Jiang, "A sequential approximate programming strategy for performance-measure-based probabilistic structural design optimization," *Struct. Saf.*, vol. 30, no. 2, pp. 91–109, Mar 2008, http://dx.doi.org/10.1016/j.strusafe.2006.08.003.

[41] H. Chiti, M. Khatibinia, A. Akbarpour, and H. R. Naseri, "Reliability-Based Design optimization of concrete gravity dams using subset simulation," *Int. J. Optim. Civ. Eng.*, vol. 6, no. 3, pp. 329–348, 2016.

[42] H. Zhao, M. Zhao, and C. Zhu, "Reliability-based optimization of geotechnical engineering using the artificial bee colony algorithm," *KSCE J. Civ. Eng.*, vol. 20, no. 5, pp. 1728–1736, 2016, http://dx.doi.org/10.1007/s12205-015-0117-6.

[43] I. E. Zevgolis, A. V. Deliveris, and N. C. Koukouzas, "Probabilistic design optimization and simplified geotechnical risk analysis for large open pit excavations," *Comput. Geotech.*, vol. 103, no. April, pp. 153–164, Nov 2018, http://dx.doi.org/10.1016/j.compgeo.2018.07.024.

[44] H. Zhao, Z. Ru, and C. Zhu, "Reliability-based Support Optimization of Rockbolt Reinforcement around Tunnels in Rock Masses," *Period. Polytech. Civ. Eng.*, vol. 62, no. 1, pp. 250–258, Sep 2017, http://dx.doi.org/10.3311/PPci.10420.

[45] M. G. C. Santos, J. L. Silva, and A. T. Beck, "Reliability-based design optimization of geosynthetic-reinforced soil walls," *Geosynth. Int.*, vol. 25, no. 4, pp. 442–455, 2018, http://dx.doi.org/10.1680/jgein.18.00028.

[46] J. Ji, C. Zhang, Y. Gao, and J. Kodikara, "Reliability-based design for geotechnical engineering: An inverse FORM approach for practice," *Comput. Geotech.*, vol. 111, pp. 22–29, Jul 2019, http://dx.doi.org/10.1016/j.compgeo.2019.02.027.

[47] K. V. N. S. Raviteja and B. M. Basha, "Reliability based LRFD of geomembrane liners for v-shaped anchor trenches of MSW landfills," *Int. J. Geosynth. Gr. Eng.*, vol. 4, no. 1, pp. 5, Mar 2018, http://dx.doi.org/10.1007/s40891-017-0123-5.

[48] C. L. Rodríguez, "Reliability-based design and topology optimization of aerospace components and structures," Ph.D. dissertation, University of Coruña, Coruña, 2016.

[49] H. H. Hilton and M. Feigen, "Minimum weight analysis based on structural reliability," *J. Aerosp. Sci.*, vol. 27, no. 9, pp. 641–652, Sep 1960, http://dx.doi.org/10.2514/8.8702.

[50] R. H. Lopez and A. T. Beck, "Reliability-based design optimization strategies based on FORM: a review," *J. Braz. Soc. Mech. Sci. Eng.*, vol. 34, no. 4, pp. 506–514, Dec 2012, http://dx.doi.org/10.1590/S1678-58782012000400012.

[51] Z. Hu and X. Du, "Lifetime cost optimization with time-dependent reliability," *Eng. Optim.*, vol. 46, no. 10, pp. 1389–1410, Oct 2014, http://dx.doi.org/10.1080/0305215X.2013.841905.

[52] A. T. Beck "Structural optimization under uncertainties: understanding the role of expected consequences of failure," in *Soft Computing Methods for Civil and Structural Engineering*, Y. Tsompanakis and B. Topping, eds. Kippen, Scotland: Saxe-Coburg Publications, 2013, ch. 5.

[53] A. J. Torii, R. H. Lopez, A. T. Beck, and L. F. F. Miguel, "A performance measure approach for risk optimization," *Struct. Multidiscipl. Optim.*, vol. 60, no. 3, pp. 927–947, Sep 2019, http://dx.doi.org/10.1007/s00158-019-02243-5.

[54] H. M. Kroetz, M. Moustapha, A. T. Beck, and B. Sudret, "A two-level kriging-based approach with active learning for solving time-variant risk optimization problems," *Reliab. Eng. Syst. Saf.*, vol. 203, pp. 107033, Nov 2020., http://dx.doi.org/10.1016/j.ress.2020.107033.

[55] N. Kuschel and R. Rackwitz, "Optimal design under time-variant reliability constraints," *Struct. Saf.*, vol. 22, no. 2, pp. 113–127, Jun 2000, http://dx.doi.org/10.1016/S0167-4730(99)00043-0.

[56] H. Streicher and R. Rackwitz, "Time-variant reliability-oriented structural optimization and a renewal model for life-cycle costing," *Probab. Eng. Mech.*, vol. 19, no. 1–2, pp. 171–183, Jan 2004., http://dx.doi.org/10.1016/j.probengmech.2003.11.014.

[57] H. Agarwal, J. Renaud, J. Lee, and L. Watson "A unilevel method for reliability based design optimization," in *45th AIAA/ASME/ASCE/AHS/ASC Structures, Structural Dynamics Mater. Conf.*, 2004, vol. 7, pp. 5374–5392, http://dx.doi.org/10.2514/6.2004-2029.

[58] Maplesoft, *Maple User Manual*. Waterloo: Maplesoft, 2020.

[59] L. Bernardin et al., *Maple Programming Guide*, Waterloo: Maplesoft, 2020.

[60] C. Corns, S. Glenn, and K. Ernest, "Gravity dam design and analysis," in *Gravity Dam Design and Analysis*, R. B. Jansen, V. N. Reinhold, eds. Boston, MA. USA: Springer, 1988, pp. 466–492.

[61] ICOLD, *Bulletin 117: The Gravity Dam: a Dam for the Future - Review and Recommendations*," Paris, France: Commission Internationale des Grand Barrages, 2000.

[62] Bureau of Indian Standards, *Code of practice for drainage system for gravity dams, their foundations and abutments*, New Delhi, 1985.

[63] F. W. Hannah and R. C. Kennedy, *The Design of Dams*. 2nd ed. New York: McGraw-Hill, 1938.

[64] R. B. Jansen, *Advanced Dam Engineering for Design, Construction, and Rehabilitation.* New York: Van Nostrand Reinhold, 1988.

[65] M. A. El-razek and M. M. A. Elela, "Optimal position of drainage gallery underneath gravity dam," in *6th Int. Water Technol. Conf.*, 2001, pp. 181–192.

[66] A. S. Chawla, R. K. Thakur, and A. Kumar, "Optimum location of drains in concrete dams," *J. Hydraul. Eng.*, vol. 116, no. 7, pp. 930–943, Jul 1990, http://dx.doi.org/10.1061/(ASCE)0733-9429(1990)116:7(930).

[67] B. Nourani, F. Salmasi, A. Abbaspour, and B. Oghati Bakhshayesh, "Numerical investigation of the optimum location for vertical drains in gravity dams," *Geotech. Geol. Eng.*, vol. 35, no. 2, pp. 799–808, Apr 2017, http://dx.doi.org/10.1007/s10706-016-0144-1.

[68] Y. Chen, C. Zhou, and H. Zheng, "A numerical solution to seepage problems with complex drainage systems," *Comput. Geotech.*, vol. 35, no. 3, pp. 383–393, May 2008, http://dx.doi.org/10.1016/j.compgeo.2007.08.005.

[69] T. Daghestani, M. Calamak, and A. M. Yanmaz, "On the optimum layout of a drainage gallery in concrete gravity dams on isotropic foundation," *Environ. Eng. Geosci.*, vol. 25, no. 4, pp. 345–358, Nov 2019, http://dx.doi.org/10.2113/EEG-2206.

[70] C.-H. Zee, R. Zee, and R. Zee, "Pore pressures in concrete dams," *J. Geotech. Geoenviron. Eng.*, vol. 137, no. 12, pp. 1254–1264, Dec 2011, http://dx.doi.org/10.1061/(ASCE)GT.1943-5606.0000536.

[71] Chinese Ministry of Hydroelectric Power, *Guideline for Design of Concrete Gravity Dams.* Bejing, China, 2005.

[72] B. M. Das, *Principles of Geotechnical Engineering*, 8th ed. United States of America: Christopher M. Shortt, 2014.

[73] JCSS, "Probabilistic Model Code, Part I - Basis of design*"*. https://www.jcss-lc.org/jcss-probabilistic-model-code/ (accessed Aug. 26, 2021).

[74] K. O. Pires, A. T. Beck, T. N. Bittencourt, and M. M. Futai, "Reliability analysis of built concrete dam," *Rev. IBRACON Estrut. Mater.*, vol. 12, no. 3, pp. 551–579, Jun 2019, http://dx.doi.org/10.1590/s1983-41952019000300007.

[75] N. Mao, T. Al-Bittar, and A.-H. Soubra, "Probabilistic analysis and design of strip foundations resting on rocks obeying Hoek–Brown failure criterion," *Int. J. Rock Mech. Min. Sci.*, vol. 49, pp. 45–58, Jan 2012, http://dx.doi.org/10.1016/j.ijrmms.2011.11.005.

[76] A. H. Alavi and E. Sadrossadat, "New design equations for estimation of ultimate bearing capacity of shallow foundations resting on rock masses," *Geosci. Frontiers*, vol. 7, no. 1, pp. 91–99, Jan 2016, http://dx.doi.org/10.1016/j.gsf.2014.12.005.

[77] C. W. Duncan, *Foundations on Rock*. 2nd ed. London/New York: E&FN SPON, 1999.

[78] A. T. Siacara, A. T. Beck, and M. M. Futai, "Reliability analysis of rapid drawdown of an earth dam using direct coupling," *Comput. Geotech.*, vol. 118, pp. 103336, Feb 2020, http://dx.doi.org/10.1016/j.compgeo.2019.103336.

[79] A. T. Siacara, G. F. Napa-García, A. T. Beck, and M. M. Futai, "Reliability analysis of earth dams using direct coupling," *J. Rock Mech. Geotech. Eng.*, vol. 12, no. 2, pp. 366–380, Apr 2020, http://dx.doi.org/10.1016/j.jrmge.2019.07.012.

[80] D. G. Fredlund, H. Rahardjo, and M. D. Fredlund, *Unsaturated Soil Mechanics in Engineering Practice.* Hoboken, NJ, USA: Wiley, 2012.

[81] United States Bureau of Reclamation – USBR, *Design of Small Dams*. 3rd ed. Washington DC, USA: US Government Printing Office, 1987.

[82] K. Y. Lo and J. D. Grass, "Recent experience with safety assessment of concrete dams on rock foundations," in *Canadian Dam Safety Conf.*, 1994, pp. 231–250.

[83] Y. A. Fishman, "Stability of concrete retaining structures and their interface with rock foundations," *Int. J. Rock Mech. Min. Sci.*, vol. 46, no. 6, pp. 957–966, Sep 2009, http://dx.doi.org/10.1016/j.ijrmms.2009.05.006.

[84] M. W. Wilde and F. Johansson, "System reliability of concrete dams with respect to foundation stability: Application to a spillway," *J. Geotech. Geoenviron. Eng.*, vol. 139, no. 2, pp. 308–319, 2013, http://dx.doi.org/10.1061/(ASCE)GT.1943-5606.0000761.

[85] Naval Facilities Engineering Command, *Foundations and earth structures, NAVFAC DM7-02*, 1986.

[86] A. K. Chopra and L. Zhang, "Earthquake-induced base sliding of concrete gravity dams," *J. Struct. Eng.*, vol. 117, no. 12, pp. 3698–3719, Dec 1991, http://dx.doi.org/10.1061/(ASCE)0733-9445(1991)117:12(3698).

[87] M. Rashki, M. Miri, and M. Azhdary Moghaddam, "A new efficient simulation method to approximate the probability of failure and most probable point," *Struct. Saf.*, vol. 39, pp. 22–29, Nov 2012, http://dx.doi.org/10.1016/j.strusafe.2012.06.003.

[88] M. Rashki, M. Miri, and M. A. Moghaddam, "A simulation-based method for reliability based design optimization problems with highly nonlinear constraints," *Autom. Construct.*, vol. 47, pp. 24–36, Nov 2014, http://dx.doi.org/10.1016/j.autcon.2014.07.004.

[89] S. E. Cho, "Probabilistic assessment of slope stability that considers the spatial variability of soil properties," *J. Geotech. Geoenviron. Eng.*, vol. 136, no. 7, pp. 975–984, Jul 2010, http://dx.doi.org/10.1061/(ASCE)GT.1943-5606.0000309.

Author contributions: ATS: conceptualization, formal analysis, methodology, writing; GPP: conceptualization, review; ATB: conceptualization, formal analysis, writing, review; MMF: conceptualization, formal analysis, writing, review, funding acquisition.

Editors: Antônio Carlos dos Santos, Guilherme Aris Parsekian.